2-Deoxy-6-*O*-[2-deoxy-2-[(*R*)-3-(octadecanoyloxy)octadecanoylamino]-β-D-glucopyranosyl]-2-[(*R*)-3-hydroxyoctadecanoylamino]-α-D-glucopyranose 1-phosphate (1): Pd-black (10.0 mg) was added to a solution of **15** (11.0 mg, 5.63 μmol) in distilled THF (1.0 mL). The mixture was stirred under hydrogen (2.0 MPa) at room temperature for 18 h and then neutralized with Et_3N in THF (10%, v/v, 20.0 μL), and the Pd catalyst was removed by filtration. After removal of the solvent in vacuo, the residue was lyophilized from *t*BuOH to afford **1** as a triethylammonium salt (white solid, 7.0 mg, quant). ^{1}H NMR (500 MHz, $CDCl_3/CD_3OD$): δ= 5.47 (d, J=4.4 Hz, 1H; H-1), 5.27 (brs, 1H; β-CH of 2′-*N*-acyl), 4.62 (d, J=8.8 Hz, 1H; H-1′), 4.08 (t, J=9.8 Hz, 1H; H-5), 4.02 (d, J=12.1 Hz, 1H; β-CH of 2-*N*-acyl), 4.02 (d, J=8.6 Hz, 1H; H-2), 3.89 (d, J=11.8 Hz, 1H; H-6a), 3.83 (dd, J=11.8, 6.3 Hz, 1H; H-6b), 3.78–3.65 (m, 2H; H-3, H-2′), 3.45–3.24 (m, 4H; H-3′, H-4′, H-6′a, H-6′b), 3.23–3.16 (m, 2H; H-4, H-5′), 2.58 (t, J=6.3 Hz, 2H; α-CH_2 of 2′-*N*-acyl main chain), 2.39–2.27 (m, 4H; α-CH_2 of 2′-*N*-acyl side chain and 2-*N*-acyl), 1.76–1.15 (m, 84H; CH_2 of 2-*N*-acyl and 2′-*N*-acyl), 0.89 ppm (t, J=6.2 Hz, 9H; -CH_2-CH_3 of 2-*N*-acyl and 2′-*N*-acyl); HRMS (ESI-Q-TOF, negative): *m/z*: calcd. for $C_{66}H_{127}N_2O_{17}P$ $[M-H]^-$: 1249.8794; found: 1249.8794.

2-Deoxy-6-*O*-[2-deoxy-2-[(*R*)-3-(octadecanoyloxy)octadecanoylamino]-β-D-glucopyranosyl]-2-[(*R*)-3-hydroxyoctadecanoylamino]-α-D-glucopyranose 1-(aminoethyl)phosphate (2): $Pd(OH)_2/C$ (20 wt% on carbon, 20.0 mg) was added to a solution of **17** (20.0 mg, 9.79 μmol) in distilled THF (1.0 mL), water (100 μL), and AcOH (50 μL). The mixture was stirred under hydrogen (2.0 MPa) at room temperature for 2 d and then neutralized with Et_3N in THF (10%, v/v, 20.0 μL), and Pd catalyst was removed by filtration. After removal of the solvent in vacuo, the residue was lyophilized from *t*BuOH to afford **2** as a colorless solid (11.2 mg, 89%). ^{1}H NMR (500 MHz, $CDCl_3/CD_3OD$): δ=5.47 (d, J=8.3 Hz, 1H; H-1), 5.26–5.22 (m, 1H; β-CH of 2′-*N*-acyl), 4.62 (d, J=8.5 Hz, 1H; H-1′), 4.21 (dd, J=18.2, 8.5 Hz, 1H; H-5), 4.04 (d, J=12.1 Hz, 1H; H-6a), 3.95–3.90 (m, 2H; H-2, β-CH of 2-*N*-acyl), 3.88 (d, J=11.8 Hz, 1H; -OPO-CH_2-CH_2-), 3.81 (t, J=10.9 Hz, 1H; H-6b), 3.72–3.65 (m, 2H; H-3, -OPO-CH_2-CH_2-), 3.60–3.55 (m, 1H; H-2′), 3.48–3.20 (m, 6H; H-3′, H-4′, H-6′a, H-6′b, -OPO-CH_2-CH_2-), 3.13–3.10 (m, 1H; H-5′), 2.95 (brs, 1H; H-4), 2.56–2.42 (m, 2H; α-CH_2 of 2′-*N*-acyl main chain), 2.41–2.22 (m, 4H; α-CH_2 of 2′-*N*-acyl side chain and 2-*N*-acyl), 1.62–1.15 (m, 84H; CH_2 of 2-*N*-acyl and 2′-*N*-acyl), 0.88 ppm (brs, 9H; -CH_2-CH_3 of 2-*N*-acyl and 2′-*N*-acyl); HRMS (ESI-Q-TOF, negative): *m/z*: calcd for $C_{68}H_{132}N_3O_{17}P$ $[M-H]^-$: 1292.9216; found: 1292.9211.

2-Deoxy-6-*O*-[2-deoxy-6-*O*-(3-deoxy-α-D-*manno*-oct-2-ulopyranosid)onic acid]-2-[(*R*)-3-(octadecanoyloxy)octadecanoylamino]-β-D-glucopyranosyl]-2-[(*R*)-3-benzyloxyoctadecanoylamino]-α-D-glucopyranose 1-phosphate (3): Pd-black (6.0 mg) was added to a solution of **23** (6.3 mg, 2.70 μmol) in distilled THF (500 μL). The mixture was stirred under hydrogen (2.0 MPa) at room temperature for 5 d and then neutralized with Et_3N in THF (10%, v/v, 20.0 μL), and Pd catalyst was removed by filtration. After removal of the solvent in vacuo, the residue was lyophilized from *t*BuOH to afford **3** as a triethylammonium salt (white solid, 4.3 mg, quant). ^{1}H NMR (600 MHz, $CDCl_3/CD_3OD$): δ=5.48 (brs, 1H; H-1), 5.26–5.18 (m, 1H; β-CH of 2′-*N*-acyl), 4.46–4.40 (m, 1H; H-1′), 4.08–3.92 (m, 5H; H-2, H-5, H-4″, H-7″, β-CH of 2-*N*-acyl), 3.84–3.56 (m, 9H; H-3, H-6a, H-6b, H-2′, H-5′, H-5″, H-6″, H-8″a, H-8″b), 3.51–3.42 (m, 3H; H-3′, H-6′a, H-6′b), 3.38–3.26 (m, 2H; H-4, H-4′), 2.56–2.50 (m, 2H; α-CH_2 of 2′-*N*-acyl main chain), 2.42–2.26 (m, 4H; α-CH_2 of 2′-*N*-acyl side chain and 2-*N*-acyl), 2.10–2.04 (m, 1H; H-3″a), 1.92–1.84 (m, 1H; H-3″b), 1.78–1.14 (m, 84H; CH_2 of 2-*N*-acyl and 2′-*N*-acyl), 0.89 ppm (t, J=7.2 Hz, 9H; -CH_2-CH_3 of 2-*N*-acyl and 2′-*N*-acyl); HRMS (ESI-Q-TOF, negative): *m/z*: calcd for $C_{74}H_{139}N_2O_{24}P$ $[M-H]^-$: 1469.9377; found: 1469.9371.

2-Deoxy-6-*O*-[2-deoxy-6-*O*-(3-deoxy-α-D-*manno*-oct-2-ulopyranosid)onic acid]-2-[[(*R*)-3-(octadecanoyloxy)octadecanoylamino]-β-D-glucopyranosyl]-2-[(*R*)-3-benzyloxyoctadecanoylamino]-α-D-glucopyranose 1-(aminoethyl)phosphate (4): $Pd(OH)_2/C$ (20 wt% on carbon, 1.0 mg) was added to a solution of **25** (1.3 mg, 0.495 μmol) in distilled THF (435 μL), water (43 μL), and AcOH (22 μL). The mixture was stirred under hydrogen (2.0 MPa) at room temperature for 2 d and then neutralized with Et_3N in THF (10%, v/v, 20.0 μL), and Pd catalyst was removed by filtration. After removal of the solvent in vacuo, the residue was washed with *n*-hexane and water and then was lyophilized from *t*BuOH to afford **4** as a white solid (110 μg, 15%). ^{1}H NMR is shown in the Supporting Information. HRMS (ESI-Q-TOF, negative): *m/z*: calcd for $C_{76}H_{144}N_3O_{24}P$ $[M-H]^-$: 1512.9799; found: 1512.9792.

Cytokine assay: The cytokine-inducing activities of the synthetic lipid A compounds and LPS (*E. coli* O111:B4, Sigma–Aldrich as a positive control) were tested in heparinized human peripheral whole blood (HPWB) cells collected from the blood of an adult volunteer. The synthesized samples (dissolved in 25 μL of 5% DMSO in saline) and HPWB (25 μL) in RPMI1640 medium (75 μL) including meylon (3%), were incubated in triplicate in a 96-well plastic plate at 37°C under CO_2 (5%). To maintain the solubility of the synthetic compounds this culture included DMSO (1%).[54] After 20 h of incubation and subsequent centrifugal separation (at 300*g* for 2 min), the supernatant proteins were collected and the induced quantities of cytokines were then measured by ELISA assay (ELISA Ready-SET-Go! (*e*Bioscience) for human IL-1β, IL-6, IL-12p70, IL-8, and TNF-α; Human IL-18 ELISA Kit (MBL) for human IL-18). For the inhibitory activities of the synthetic lipid A compounds and Kdo-lipid A compounds against *E. coli* LPS, the synthetic compounds and additional *E. coli* LPS (500 pg mL^{-1}) in RPMI 1640 medium including meylon (3%) and a buffer solution were incubated and measured by a method similar to that used for the inducing activities. Data represent averages of three repeated assays with standard deviations from individual experiments.

Acknowledgements

This work was supported in part by Grants-in Aid for Scientific Research (Nos. 22310136, 20241053, 19310144, 17310128, and 20–870) and the NEXT program from the Japan Society for the Promotion of Science, as well as by grants from Osaka University Global COE program (Frontier Biomedical Science Underlying Organelle Network Biology), the Naito Foundation, and the Takeda Science Foundation. The authors would also like to acknowledge Prof. Yasuhiro Kajihara, Seiji Adachi, and Naoya Inazumi of Osaka University for the NMR measurements and fruitful discussions.

[1] P. B. Ernst, B. D. Gold, *Annu. Rev. Microbiol.* **2000**, *54*, 615–640.
[2] R. M. Peek, Jr., J. E. Crabtree, *J. Pathol.* **2006**, *208*, 233–248.
[3] P. B. Ernst, D. A. Peura, S. E. Crowe, *Gastroenterology* **2006**, *130*, 188–206; P. B. Ernst, D. A. Peura, S. E. Crowe, *Gastroenterology* **2006**, *130*, 212–213.
[4] S. O. Hynes, J. A. Ferris, B. Szponar, T. Wadstrom, J. G. Fox, J. O'Rourke, L. Larsson, E. Yaquian, A. Ljungh, M. Clyne, L. P. Andersen, A. P. Moran, *Helicobacter* **2004**, *9*, 313–323.
[5] H. Nielsen, S. Birkholz, L. P. Andersen, A. P. Moran, *J. Infect. Dis.* **1994**, *170*, 135–139.
[6] G. I. Perez-Perez, V. L. Shepherd, J. D. Morrow, M. J. Blaser, *Infect. Immun.* **1995**, *63*, 1183–1187.
[7] S. Yokota, H. Saito, T. Kubota, N. Yokosawa, K. Amano, N. Fujii, *Virology* **2003**, *306*, 135–146.
[8] S. W. Montminy, N. Khan, S. McGrath, M. J. Walkowicz, F. Sharp, J. E. Conlon, K. Fukase, S. Kusumoto, C. Sweet, K. Miyake, S. Akira, R. J. Cotter, J. D. Goguen, E. Lien, *Nat. Immunol.* **2006**, *7*, 1066–1073.
[9] R. Ross, *N. Engl. J. Med.* **1999**, *340*, 115–126.
[10] J. Danesh, R. Collins, R. Peto, *Lancet* **1997**, *350*, 430–436.
[11] J. Danesh, Y. Wong, M. Ward, J. Muir, *Heart* **1999**, *81*, 245–247.
[12] C. C. Kuo, J. T. Grayston, L. A. Campbell, Y. A. Goo, R. W. Wissler, E. P. Benditt, *Proc. Natl. Acad. Sci. USA* **1995**, *92*, 6911–6914.
[13] J. T. Grayston, *J. Infect. Dis.* **2000**, *181 Suppl 3*, S402–410.
[14] A. Schumacher, I. Seljeflot, A. B. Lerkerod, L. Sommervoll, J. E. Otterstad, H. Arnesen, *Atherosclerosis* **2002**, *164*, 153–160.
[15] G. Hajishengallis, A. Sharma, M. W. Russell, R. J. Genco, *Ann. Periodontol.* **2002**, *7*, 72–78.

[16] F. C. Gibson III, H. Yumoto, Y. Takahashi, H. H. Chou, C. A. Genco, *J. Dent. Res.* **2006**, *85*, 106–121.
[17] G. A. Roth, B. Moser, F. Roth-Walter, M. B. Giacona, E. Harja, P. N. Papapanou, A. M. Schmidt, E. Lalla, *Atherosclerosis* **2007**, *190*, 271–281.
[18] F. C. Gibson III, T. Ukai, C. A. Genco, *Front. Biosci.* **2008**, *13*, 2041–2059.
[19] M. Triantafilou, F. G. Gamper, P. M. Lepper, M. A. Mouratis, C. Schumann, E. Harokopakis, R. E. Schifferle, G. Hajishengallis, K. Triantafilou, *Cell Microbiol.* **2007**, *9*, 2030–2039.
[20] K. Honjo, R. van Reekum, N. P. L. G. Verhoeff, *Alzheimer's Dementia* **2009**, *5*, 348–360.
[21] H. Okamura, H. Tsutsi, T. Komatsu, M. Yutsudo, A. Hakura, T. Tanimoto, K. Torigoe, T. Okura, Y. Nukada, K. Hattori, *Nature* **1995**, *378*, 88–91.
[22] M. Trøseid, I. Seljeflot, H. Arnesen, *Cardiovasc. Diabetol.* **2010**, *9*, 11.
[23] S. Alboni, D. Cervia, S. Sugama, B. Conti, *J. Neuroinflammation* **2010**, *7*, 9.
[24] T. Tomita, A. M. Jackson, N. Hida, M. Hayat, M. F. Dixon, T. Shimoyama, A. T. Axon, P. A. Robinson, J. E. Crabtree, *J. Infect. Dis.* **2001**, *183*, 620–627.
[25] M. T. Fera, M. Carbone, C. Buda, M. Aragona, S. Panetta, M. Giannone, F. La Torre, A. Giudice, E. Losi, *Ann. N.Y. Acad. Sci.* **2002**, *963*, 326–328.
[26] K. Yamauchi, I. J. Choi, H. Lu, H. Ogiwara, D. Y. Graham, Y. Yamaoka, *J. Immunol.* **2008**, *180*, 1207–1216.
[27] Y. Suda, Y. Kim, K. Nagata, Y. Hasegawa, A. Kawaguchi, M. Oikawa, K. Nakajima, K. Aoyama, T. Ogawa, T. Shimoyama, T. Tamura, S. Kusumoto, *Symposium Papers: Symposium on the Chemistry of Natural Products* **2001**, *43*, 383–388.
[28] S. Kusumoto, K. Fukase, Y. Fujimoto in *Microbial Glycobiology: Structures, Relevance and Applications* (Eds.: A. Moran, O. Holst, P. J. Brennan, M. v. Itzstein), Elsevier, London, **2009**, pp. 415–427.
[29] Y. Fukase, Y. Fujimoto, Y. Adachi, Y. Suda, S. Kusumoto, K. Fukase, *Bull. Chem. Soc. Japan* **2008**, *81*, 796–819.
[30] Y. Fujimoto, Y. Adachi, M. Akamatsu, Y. Fukase, M. Kataoka, Y. Suda, K. Fukase, S. Kusumoto, *J. Endotoxin Res.* **2005**, *11*, 341–347.
[31] Y. Fujimoto, M. Iwata, N. Imakita, A. Shimoyama, Y. Suda, S. Kusumoto, K. Fukase, *Tetrahedron Lett.* **2007**, *48*, 6577–6581.
[32] Y. Suda, T. Ogawa, W. Kashihara, M. Oikawa, T. Shimoyama, T. Hayashi, T. Tamura, S. Kusumoto, *J. Biochem.* **1997**, *121*, 1129–1133.
[33] A. P. Moran, B. Lindner, E. J. Walsh, *J. Bacteriol.* **1997**, *179*, 6453–6463.
[34] Y. Sakai, M. Oikawa, H. Yoshizaki, T. Ogawa, Y. Suda, K. Fukase, S. Kusumoto, *Tetrahedron Lett.* **2000**, *41*, 6843–6847.
[35] N. Sawada, T. Ogawa, Y. Asai, Y. Makimura, A. Sugiyama, *Clin. Exp. Immunol.* **2007**, *148*, 529–536.
[36] H. Kumada, Y. Haishima, K. Watanabe, C. Hasegawa, T. Tsuchiya, K. Tanamoto, T. Umemoto, *Oral Microbiol. Immunol.* **2008**, *23*, 60–69.
[37] Y. Zhang, J. Gaekwad, M. A. Wolfert, G. J. Boons, *Org. Biomol. Chem.* **2008**, *6*, 3371–3381.
[38] K. Fukase, Y. Fukase, M. Oikawa, W. C. Liu, Y. Suda, S. Kusumoto, *Tetrahedron* **1998**, *54*, 4033–4050.
[39] Y. H. Zhang, J. Gaekwad, M. A. Wolfert, G. J. Boons, *J. Am. Chem. Soc.* **2007**, *129*, 5200–5216.
[40] Y. Zhang, J. Gaekwad, M. A. Wolfert, G. J. Boons, *Chem. Eur. J.* **2008**, *14*, 558–569.
[41] S. Inamura, K. Fukase, S. Kusumoto, *Tetrahedron Lett.* **2001**, *42*, 7613–7616.
[42] I. Shiina, H. Ushiyama, Y.-k. Yamada, Y.-i. Kawakita, K. Nakata, *Chem. Asian J.* **2008**, *3*, 454–461.
[43] A. Merzouk, F. Guibe, A. Loffet, *Tetrahedron Lett.* **1992**, *33*, 477–480.
[44] D. Baudry, M. Ephritikhine, H. Felkin, *J. Chem. Soc. Chem. Commun.* **1978**, 694–695.
[45] M. Inage, H. Chaki, S. Kusumoto, T. Shiba, *Chem. Lett.* **1982**, 1281–1284.
[46] A. Campbell, B. Fraser-Reid, *Bioorg. Med. Chem.* **1994**, *2*, 1209–1219.
[47] G. D. Prestwich, J. F. Marecek, R. J. Mourey, A. B. Theibert, C. D. Ferris, S. K. Danoff, S. H. Snyder, *J. Am. Chem. Soc.* **1991**, *113*, 1822–1825.
[48] R. W. Murray, R. Jeyaraman, *J. Org. Chem.* **1985**, *50*, 2847–2853.
[49] H. Yoshizaki, N. Fukuda, K. Sato, M. Oikawa, K. Fukase, Y. Suda, S. Kusumoto, *Angew. Chem.* **2001**, *113*, 1523–1528; *Angew. Chem. Int. Ed.* **2001**, *40*, 1475–1480.
[50] B. Yu, H. Tao, *Tetrahedron Lett.* **2001**, *42*, 2405–2407.
[51] H. Tokimoto, Y. Fujimoto, K. Fukase, S. Kusumoto, *Tetrahedron: Asymmetry* **2005**, *16*, 441–447.
[52] K. Watanabe, N. Yamagiwa, Y. Torisawa, *Org. Process Res. Dev.* **2007**, *11*, 251–258.
[53] T. Goi, K. Tanaka, K. Fukase, *J. Carbohydr. Chem.* **2007**, *26*, 369–394.
[54] Y. Suda, H. Tochio, K. Kawano, H. Takada, T. Yoshida, S. Kotani, S. Kusumoto, *FEMS Immunol. Med. Microbiol.* **1995**, *12*, 97–112.
[55] T. Ogawa, Y. Asai, Y. Sakai, M. Oikawa, K. Fukase, Y. Suda, S. Kusumoto, T. Tamura, *FEMS Immunol. Med. Microbiol.* **2003**, *36*, 1–7.
[56] M. Mueller, B. Lindner, S. Kusumoto, K. Fukase, A. B. Schromm, U. Seydel, *J. Biol. Chem.* **2004**, *279*, 26307–26313.
[57] J. Gaekwad, Y. H. Zhang, W. Zhang, J. Reeves, M. A. Wolfert, G. J. Boons, *J. Biol. Chem.* **2010**, *285*, 29375–29386.
[58] H. Tsutsui, T. Yoshimoto, N. Hayashi, H. Mizutani, K. Nakanishi, *Immunol. Rev.* **2004**, *202*, 115–138.
[59] K. Nakanishi, T. Yoshimoto, H. Tsutsui, H. Okamura, *Annu. Rev. Immunol.* **2001**, *19*, 423–474.
[60] H. Okamura, S. Kashiwamura, H. Tsutsui, T. Yoshimoto, K. Nakanishi, *Curr. Opin. Immunol.* **1998**, *10*, 259–264.
[61] M. Imamura, H. Tsutsui, K. Yasuda, R. Uchiyama, S. Yumikura-Futatsugi, K. Mitani, S. Hayashi, S. Akira, S. Taniguchi, N. Van Rooijen, J. Tschopp, T. Yamamoto, J. Fujimoto, K. Nakanishi, *J. Hepatol.* **2009**, *51*, 333–341.
[62] T. D. Kanneganti, M. Lamkanfi, Y. G. Kim, G. Chen, J. H. Park, L. Franchi, P. Vandenabeele, G. Nuñez, *Immunity* **2007**, *26*, 433–443.
[63] T. Kawai, S. Akira, *Int. Immunol.* **2009**, *21*, 317–337.
[64] M. Krummen, S. Balkow, L. Shen, S. Heinz, C. Loquai, H. C. Probst, S. Grabbe, *J. Leukocyte Biol.* **2010**, *88*, 189–199.
[65] Y. Chen, M. J. Blaser, *J. Infect. Dis.* **2008**, *198*, 553–560.
[66] M. Vasan, M. A. Wolfert, G. J. Boons, *Org. Biomol. Chem.* **2007**, *5*, 2087–2097.
[67] Y. H. Zhang, M. A. Wolfert, G. J. Boons, *Bioorg. Med. Chem.* **2007**, *15*, 4800–4812.

Received: December 11, 2010
Revised: July 27, 2011
Published online: November 16, 2011

A more efficient method to generate integration-free human iPS cells

Keisuke Okita[1], Yasuko Matsumura[1], Yoshiko Sato[1], Aki Okada[1], Asuka Morizane[1,2], Satoshi Okamoto[3], Hyenjong Hong[1], Masato Nakagawa[1], Koji Tanabe[1], Ken-ichi Tezuka[4], Toshiyuki Shibata[5], Takahiro Kunisada[4], Masayo Takahashi[1,3], Jun Takahashi[1,2], Hiroh Saji[6] & Shinya Yamanaka[1,7–9]

We report a simple method, using p53 suppression and nontransforming L-Myc, to generate human induced pluripotent stem cells (iPSCs) with episomal plasmid vectors. We generated human iPSCs from multiple donors, including two putative human leukocyte antigen (HLA)-homozygous donors who match ~20% of the Japanese population at major HLA loci; most iPSCs are integrated transgene-free. This method may provide iPSCs suitable for autologous and allologous stem-cell therapy in the future.

Genomic integration of transgenes increases the risk of tumor formation and mortality in chimeric and progeny mice derived from induced pluripotent stem cells (iPSCs)[1]. Integration-free human iPSCs have been generated using several methods, including adenovirus[2], Sendai virus[3], the piggyBac system[4], minicircle vector[5], episomal vectors[6], direct protein delivery[7] and synthesized mRNA[8] (**Supplementary Table 1**). However, reprogramming efficiency using integration-free methods is impractically low in most cases. Direct delivery of proteins or RNA is labor-intensive, requiring repeated delivery of the reprogramming factors. Modifying Sendai virus vectors or preparing synthesized RNA are technically demanding.

In the original report describing episomal plasmid vectors for reprogramming, the authors used seven factors, including *POU5F1* (also known as *OCT3/4*), *SOX2*, *KLF4*, *MYC* (also known as *c-MYC*), *NANOG*, *LIN28A* (also known as *LIN28*) and SV40 large T antigen (*SV40LT*), in three different vector combinations[6] (T1–T3 combinations; **Fig. 1a** and **Supplementary Table 2**). In this study, we used two findings from our laboratory to enhance efficiency of reprogramming by episomal plasmids: iPSC generation is markedly enhanced by p53 suppression[9], and L-Myc is more potent and specific than c-Myc during human iPSC generation[10].

We prepared four vector combinations (**Fig. 1a** and **Supplementary Table 2**). The Y1 combination had six factors (*OCT3/4*, *SOX2*, *KLF4*, *c-MYC*, *LIN28* and *NANOG*) in three episomal plasmids. The Y2 combination contained an additional *TP53* (also known as *p53*) shRNA in one of the three plasmids. We replaced *c-MYC* and *NANOG* with *MYCL1* (also known as *L-MYC*) in the Y1 and Y2 combinations, respectively, to yield the Y3 and Y4 combinations (**Fig. 1b**).

We electroporated these seven combinations of episomal vectors (Y1–Y4 or T1–T3) into three human dermal fibroblast (HDF) lines and two dental pulp cell lines on day 0 (**Fig. 1c**). We trypsinized transfected cells on day 7 and reseeded them onto feeder layers. We maintained the cells in embryonic stem cell (ESC) medium, and small cell colonies became visible ~2 weeks after transfection. We counted the number of colonies with a flat human ESC–like morphology and non-ESC-like colonies around day 30 (**Supplementary Fig. 1**). The Y4 combination resulted in significantly ($P < 0.05$) more iPSC colonies than did any of T1–T3 combinations (**Fig. 1d**). In addition to these five parental cell lines, we obtained iPSC colonies from seven additional HDF lines with the Y4 combination of factors (**Supplementary Table 3**).

We expanded ESC-like colonies derived with the Y4 combination for additional experiments. The majority of the colonies were expandable and exhibited a cellular morphology similar to that of human ESCs, characterized by large nuclei and scant cytoplasm (**Fig. 2a,b**). We termed these episomal plasmid vector-derived iPSCs 'pla-iPSCs'. Ten of eleven clones we analyzed were karyotypically normal (**Supplementary Fig. 2** and **Supplementary Table 4**). Short tandem repeat analyses confirmed that pla-iPSC clones were derived from HDFs and dental pulp cells (**Supplementary Table 5**). Reverse transcription–PCR (RT-PCR) analyses revealed that pla-iPSC clones expressed pluripotent stem cell markers, such as *OCT3/4*, *SOX2*, *NANOG* and *DPPA5*, at levels comparable to those in ESCs and retrovirus-derived iPSC clones (**Fig. 2c** and **Supplementary Figs. 3a, 4** and **5**). Global gene expression profiles also showed that pla-iPSC clones were similar to ESC and retro-iPSC clones (**Supplementary Fig. 6** and **Supplementary Table 6**). The DNA methylation levels of CpG sites in the promoter region of *NANOG* were high in parental HDFs and dental pulp cells but were low in pla-iPSCs and ESCs (**Fig. 2d**).

To examine whether episomal vectors persisted in pla-iPSCs, first we transfected an episomal vector encoding enhanced GFP

[1]Center for iPS Cell Research and Application, Kyoto University, Kyoto, Japan. [2]Department of Biological Repair, Institute for Frontier Medical Sciences, Kyoto University, Kyoto, Japan. [3]Laboratory for Retinal Regeneration, Center for Developmental Biology, RIKEN, Kobe, Japan. [4]Department of Tissue and Organ Development, Gifu University Graduate School of Medicine, Gifu, Japan. [5]Department of Oral and Maxillofacial Science, Gifu University Graduate School of Medicine, Gifu, Japan. [6]Human Leukocyte Antigen (HLA) Laboratory, Kyoto, Japan. [7]Institute for Integrated Cell-Material Sciences, Kyoto University, Kyoto, Japan. [8]Yamanaka Induced Pluripotent Stem Cell Project, Japan Science and Technology Agency, Kawaguchi, Japan. [9]Gladstone Institute of Cardiovascular Disease, San Francisco, California, USA. Correspondence should be addressed to K.O. (okita@cira.kyoto-u.ac.jp) or S.Y. (yamanaka@cira.kyoto-u.ac.jp).

RECEIVED 29 OCTOBER 2010; ACCEPTED 8 FEBRUARY 2011; PUBLISHED ONLINE 3 APRIL 2011; DOI:10.1038/NMETH.1591

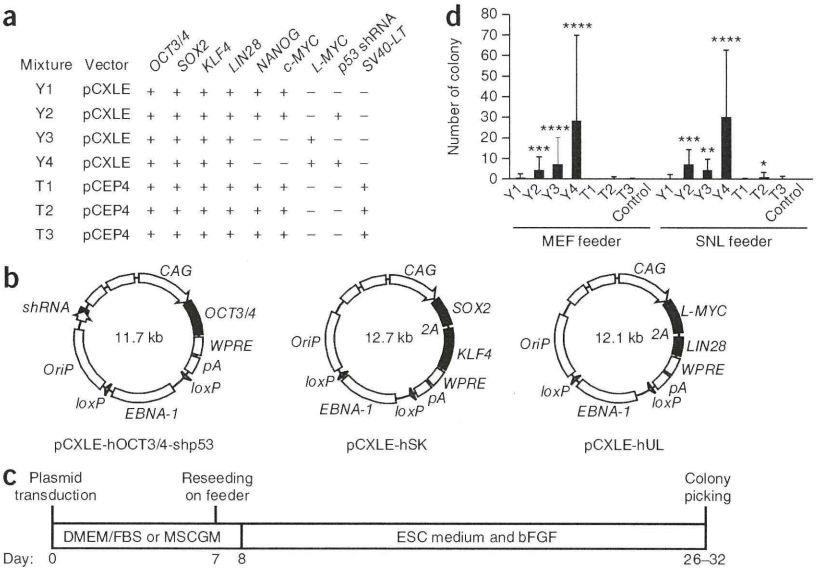

Figure 1 | Establishment of human iPSCs. (**a**) Combinations of reprogramming factors and episomal vectors used in this study. (**b**) Episomal expression vectors in the Y4 combination. *CAG*, CAG promoter; *WPRE*, woodchuck hepatitis post-transcriptional regulatory element; and *pA*, polyadenylation signal. (**c**) Schematic of the pla-iPSC induction protocol. DMEM, Dulbecco's modified Eagle medium; FBS, fetal bovine serum; MSCGM, mesenchymal stem cell growth medium; bFGF, basic fibroblast growth factor. (**d**) Numbers of colonies per 1.0×10^5 cells obtained with different combinations of reprogramming factors. Control, cells transduced with episomal vector encoding EGFP; MEF, mouse embryonic fibroblasts; SNL, mouse embryonic fibroblast cell line. Data are means ± s.d. of numbers of ESC-like colonies obtained from 15 independent induction experiments using five cell lines. $^{****}P < 0.05$ against T1, T2, T3 and control; $^{***}P < 0.05$ against T1, T3 and control; $^{**}P < 0.05$ against T1 and control; $^{*}P < 0.05$ against control.

(EGFP) into fibroblasts and monitored fluorescence. Sixty-eight percent of the cells were fluorescent 1 week after transfection (**Supplementary Fig. 7**). However, the signal quickly decreased thereafter, and only 2.4% of cells were fluorescent 4 weeks after electroporation. Then we estimated the copy numbers of the episomal vectors in established pla-iPSC clones. We designed a PCR primer pair for *EBNA-1* sequence derived from Epstein-Barr virus to calculate the copy numbers of the episomal vectors and another primer pair for the endogenous *FBXO15* locus to estimate the cell number. We detected ~200 copies of the episomal vectors per cell 6 d after transfection (**Fig. 2e** and **Supplementary Fig. 3b**). In contrast, we detected no *EBNA-1* DNA in five of seven clones tested at passages 11–20 (~80–120 d after transfection). The remaining two clones contained ~0.001 and 2 copies, respectively. The latter clone likely had integrated the plasmid into a chromosome.

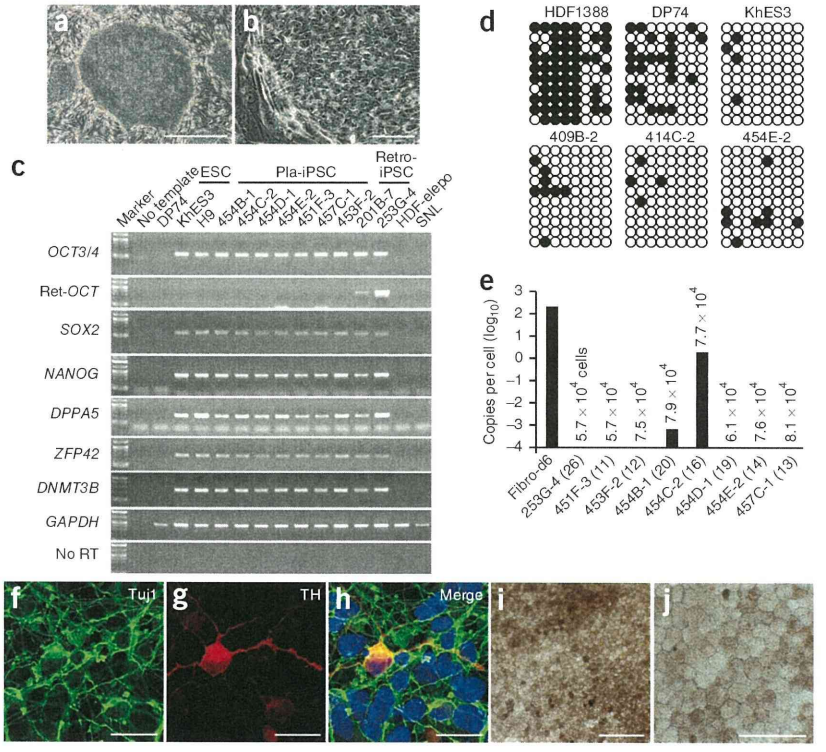

Figure 2 | Characterization of pla-iPSC clones. (**a**,**b**) Phase contrast images of an established pla-iPSC line. Scale bars, 1 mm (**a**) and 100 μm (**b**). (**c**) RT-PCR analyses for pluripotent cell markers. Total RNA was isolated from pla-iPSC clones established with the Y1 (clone 454B-1), Y2 (454C-2), Y3 (454D-1) or Y4 (454E-2, 451F-3, 457C-1 and 453F-2) combinations, from retrovirus-derived iPSC clones (retro-iPSC) and from ESC lines. In the lanes labeled *OCT3/4* and *SOX2*, PCR primers only detected endogenous gene expression; in the Ret-*OCT* lane, PCR primers specifically amplified the retroviral *OCT3/4* transgene. *GAPDH* was used as a loading control. As a negative control, *GAPDH* amplification was also performed without reverse transcription (no RT). Fibroblasts 4 d after electroporation of the Y4 mixture (HDF-elepo) and mouse embryonic fibroblast cell line (SNL) were used as other negative controls. (**d**) DNA methylation status of the *NANOG* promoter region in the indicated cell lines. Open and closed circles indicate unmethylated and methylated CpG dinucleotides, respectively. (**e**) Copy numbers of episomal vectors in pla-iPSC clones. Numbers in parentheses indicate passage number. Also shown are the estimated numbers of cells analyzed for each clone. Fibroblasts 6 d after electroporation of the Y4 combination were analyzed (fibro-d6) as a positive control. (**f**–**h**) Differentiation of pla-iPSC clone (454E-2) into dopaminergic neurons. Micrographs are immunostained for Tuj1 (**f**) and tyrosine hydroxylase (TH) (**g**). A merged image with nuclear staining using DAPI (**h**) is shown. Scale bars, 20 μm. (**i**,**j**) Differentiation of pla-iPS clone (454E-2) into retinal pigment epithelial cells. Scale bars, 100 μm (**i**) and 50 μm (**j**).

These data demonstrated that the episomal vectors were spontaneously lost in the majority of pla-iPSC clones.

We examined the differentiation potential of pla-iPSCs *in vivo*. Injection of pla-iPSCs into the testes of immunodeficient mice yielded tumors within 3 months. Histological examination confirmed that these tumors were teratomas and contained tissues of all three germ layers, including neural epithelium, cartilage and gut-like epithelium (**Supplementary Fig. 8**).

We carried out directed differentiation of the pla-iPSCs into dopaminergic neurons *in vitro* (Online Methods). RT-PCR detected upregulation of *SOX1*, a marker of immature neural cells, and downregulation of *OCT3/4* 12 d after induction (**Supplementary Fig. 9a**). Immunostaining showed that the majority of cells expressed Nestin after 29 d, with some cells still proliferating and expressed Ki67 (**Supplementary Fig. 9b–e**). Clusters of Nestin-expressing cells expressed PAX6, and more mature cell clusters expressed tyrosine hydroxylase, a marker of dopaminergic neurons (**Supplementary Fig. 9f,g**). Tyrosine hydroxylase–expressing cells localized with the neural markers Tuj1 and MAP2ab, and the vesicular monoamine transporter VMAT2 (**Fig. 2f–h** and **Supplementary Fig. 9h–l**). Therefore, pla-iPSCs have the potential to differentiate into dopaminergic neurons.

We also examined whether pla-iPSC clones differentiated into retinal pigment epithelial cells using a modified stromal cell–derived inducing activity method (Online Methods). Five of six pla-iPSC clones developed pigmented cell clusters after 30 d in conditioning medium of mouse PA6 stromal cells. The clusters grew and exhibited a squamous and hexagonal morphology, characteristic of retinal pigment epithelial cells (**Fig. 2i,j**).

We examined the human leukocyte antigen (HLA) types of our dental pulp-derived iPSC lines. In a previous study only one HLA type had been detected in two dental pulp lines by a PCR–reverse sequence–specific oligonucleotide probe (rSSOP) protocol[11]: line DP74 had been typed as *HLA-A*24*, –; *HLA-B*52*, –; *HLA-DRB1*15*, –, and line DP94 as *HLA-A*11*, –; *HLA-B*15*, –; *HLA-DRB1*04*, – ('–' means no other allele was detected; **Supplementary Table 7**). We also typed these lines with two additional analyses. A PCR-rSSOP protocol optimized for the Japanese population typed line DP74 and its progeny iPSC lines (454E-2 and 457C-1) as *HLA-A*24:02*, –; *HLA-B*52:01*, –; *HLA-DRB1*15:02*, –, and typed DP94 and its progeny iPSC line (453F-2) as *HLA-A*11:01*, –; *HLA-B*15:01*, –; *HLA-DRB1*04:06*, –. Sequence-based typing showed that the types of DP74 and DP94 were *HLA-A*24:02:01*, –; *HLA-B*52:01:01*, –; *HLA-DRB1*15:02:01*, – and *HLA-A*11:01:01*, –; *HLA-B*15:01:01*, –; *HLA-DRB1*04:06:01*, –, respectively. The families of the donors of the two dental pulp lines could not be typed because the lines were established in an anonymous way. Therefore, it is not possible to formally conclude that these donors are homozygous for the HLA haplotypes. Nevertheless, the fact that three independent analyses detected only one type in each donor is indicative of homozygosity.

According to the HLA Laboratory database, frequencies of *HLA-A*24:02*; *HLA-B*52:01*; *HLA-DRB1*15:02* and *HLA-A*11:01*; *HLA-B*15:01*; *HLA-DRB1*04:06* haplotypes in the Japanese population are 8.5% and 1.3%, respectively (http://www.hla.or.jp/hapro_e/top.html; **Supplementary Table 8**). Theoretically, iPSCs established from these two individuals match ~20% of all the combinations of 2,117 haplotypes in Japanese population. Indeed, pla-iPSC lines derived from lines DP74 and DP94 match 32 of 107

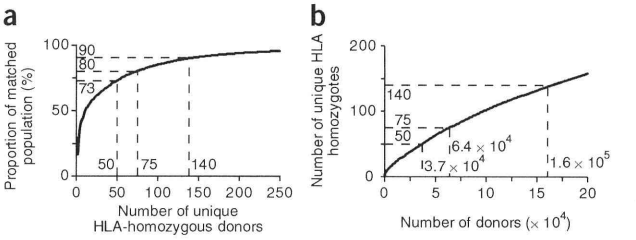

Figure 3 | Estimated coverage of the Japanese population by HLA homozygous donors. (**a**) Estimated cumulative coverage of the Japanese population by theoretical unique *HLA* homozygous donors at *HLA-A*, *HLA-B* and *HLA-DRB1* loci with four-digit specification. (**b**) Estimated numbers of donors required to identify individuals with unique HLA homozygous haplotypes.

donors[11] at the three *HLA* loci (*HLA-A*, *HLA-B* and *HLA-DR*) with the two-digit specification (**Supplementary Table 7**).

Others previously estimated that iPSC lines with 50 unique HLA homozygous haplotypes would match ~90% of the Japanese population at the *HLA-A*, *HLA-B* and *HLA-DRB1* loci with two-digit specification[12]. We performed a similar estimation with four-digit specification using the HLA Laboratory database and found that 50 unique HLA-homozygous donors would cover ~73% of the Japanese population (**Fig. 3a** and **Supplementary Table 8**). Approximately 75 and 140 unique donors would be needed to cover ~80% and 90%, respectively. It would be necessary to type ~37,000, ~64,000 and ~160,000 individuals, respectively, to identify these 50, 75 and 140 donors (**Fig. 3b**).

Allografts using *HLA*-homozygous iPSCs may provide a therapeutic alternative to autologous grafts, for cases in which transplant is likely to be needed soon after injury; furthermore, they allow for the advance selection of safe clones[13]. The beneficial effects of matching at major *HLA* loci are well documented in renal transplantation[14,15], although recipients of allografts derived from *HLA*-homozygous iPSCs would still need immunosuppressants after transplantation because of other HLA antigens, non-HLA antigens and immunity by natural killer cells.

We report a simple, non-integrative method for reprogramming human cells. The increased efficiency and the use of non-transforming Myc should be useful to generate iPSCs from many donors, such as individuals with disease. The approach may also prove beneficial for generating human iPSCs for use in autologous and allologous stem cell therapy.

METHODS

Methods and any associated references are available in the online version of the paper at http://www.nature.com/naturemethods/.

Accession codes. Addgene: 27076 (pCXLE-hOCT3/4), 27077 (pCXLE-hOCT3/4-shp53-F), 27078 (pCXLE-hSK), 27079 (pCXLE-hMLN), 27080 (pCXLE-hUL), 27081 (pCXLE-Fbx15-cont2) and 27082 (pCXLE-EGFP).

Note: Supplementary information is available on the Nature Methods website.

ACKNOWLEDGMENTS

We thank K. Takahashi, T. Aoi and Y. Yoshida for scientific discussion; M. Narita, T. Ichisaka, M. Ohuchi, M. Nishikawa and N. Takizawa for technical assistance; R. Kato, E. Nishikawa, S. Takeshima, Y. Ohtsu and H. Hasaba for administrative assistance; and H. Niwa (RIKEN) and J. Miyazaki (Osaka University) for the *CAG* promoter. This study was supported in part by a grant from the Program

for Promotion of Fundamental Studies in Health Sciences of National Institute of Biomedical Innovation, a grant from the Leading Project of Ministry of Education, Culture, Sports, Science and Technology (MEXT), a grant from Funding Program for World-Leading Innovative Research and Development on Science and Technology (FIRST Program) of Japan Society for the Promotion of Science, Grants-in-Aid for Scientific Research of Japan Society for the Promotion of Science and MEXT (to S.Y.) and Senri Life Science Foundation (to K.O.). H.H. is supported by a Japanese government (MEXT) scholarship.

AUTHOR CONTRIBUTIONS

K.O. and S.Y. conceived the project and wrote the manuscript. K.O. constructed the vectors with H.H., M.N. and K. Tanabe, and conducted most of the experiments with Y.M., Y. S. and A.O. A.M. and J.T. carried out the differentiation experiment into dopaminergic neurons. S.O. and M.T. performed differentiation into retinal pigment epithelial cells. K. Tezuka., T.S. and T.K. established dental pulp cell lines. H.S. performed HLA haplotyping in Japanese population and supervised HLA analysis.

COMPETING FINANCIAL INTERESTS

The authors declare competing financial interests: details accompany the full-text HTML version of the paper at http://www.nature.com/naturemethods/.

Published online at http://www.nature.com/naturemethods/.
Reprints and permissions information is available online at http://www.nature.com/reprints/index.html.

1. Okita, K., Ichisaka, T. & Yamanaka, S. *Nature* **448**, 313–317 (2007).
2. Zhou, W. & Freed, C.R. *Stem Cells* **27**, 2667–2674 (2009).
3. Fusaki, N., Ban, H., Nishiyama, A., Saeki, K. & Hasegawa, M. *Proc. Jpn. Acad. B* **85**, 348–362 (2009).
4. Woltjen, K. *et al. Nature* **458**, 766–770 (2009).
5. Jia, F. *et al. Nat. Methods* **7**, 197–199 (2010).
6. Yu, J. *et al. Science* **324**, 797–801 (2009).
7. Kim, D. *et al. Cell Stem Cell* **4**, 472–476 (2009).
8. Warren, L. *et al. Cell Stem Cell* **7**, 618–630 (2010).
9. Hong, H. *et al. Nature* **460**, 1132–1135 (2009).
10. Nakagawa, M., Takizawa, N., Narita, M., Ichisaka, T. & Yamanaka, S. *Proc. Natl. Acad. Sci. USA* **107**, 14152–14157 (2010).
11. Tamaoki, N. *et al. J. Dent. Res.* **89**, 773–778 (2010).
12. Nakatsuji, N., Nakajima, F. & Tokunaga, K. *Nat. Biotechnol.* **26**, 739–740 (2008).
13. Tsuji, O. *et al. Proc. Natl. Acad. Sci. USA* **107**, 12704–12709 (2010).
14. Takemoto, S.K., Terasaki, P.I., Gjertson, D.W. & Cecka, J.M. *N. Engl. J. Med.* **343**, 1078–1084 (2000).
15. Aydingoz, S.E. *et al. Hum. Immunol.* **68**, 491–499 (2007).

ONLINE METHODS

Cell culture. Human fibroblasts HDF1419, HDF1388, HDF1429, HDF1377, HDF1437 and HDF1554 were purchased from Cell Applications, and TIG121, TIG120, TIG114 and TIG107 were obtained from the Japanese Collection of Research Bioresources. Human fibroblasts were cultured in DMEM (Nacalai Tesque) supplemented with 10% FCS (Invitrogen). Human dental pulp (DP) cells were established from human third molars as described previously[11] and were maintained in mesenchymal stem cell growth medium (MSCGM; Lonza). Human ESC lines (KhES-1 and KhES-3) were obtained from Kyoto University. H1 and H9 were from WiCell Research Institute. Mouse embryonic fibroblasts (MEFs) were isolated from embryonic day 13.5 embryos of C57BL/6 mice. All mice used in this study were bred and killed appropriately following code of ethics of animal research committee in Kyoto University. MEF and mouse embryonic fibroblast cell line (SNL) cells[16] were cultured in DMEM supplemented with 7% (v/v) FCS, 2 mM L-glutamine and 50 units and 50 mg ml^{-1} penicillin and streptomycin, respectively. Established iPSCs and ESCs were maintained on mitomycin C–treated SNL cells in primate ESC medium (ReproCELL) containing 4 ng ml^{-1} of bFGF (Wako) as described previously[17].

Vector construction. Efficient transgene expression was achieved by inserting the woodchuck hepatitis post-transcriptional regulatory element (*WPRE*) upstream of the polyadenylation signal of pCX-EGFP[18]. The episomal cassette was transferred from pCEP4 (Invitrogen). The *EBNA-1* sequence (EcoRI and MfeI sites) was flanked by two *loxP* sequences, and the *loxP–EBNA-1–loxP–OriP* cassette was then digested with BamHI and BglII and inserted into the BamHI site of pCX-EGFP containing the *WPRE*. This episomal vector was designated pCXLE-EGFP.

Human cDNAs encoding *OCT3/4*, *SOX2*, *KLF4*, *c-MYC*, *L-MYC*, *NANOG* and *LIN28* were amplified by PCR and cloned into pCR2.1 (Invitrogen). The translation termination codons of *SOX2*, *c-MYC*, *L-MYC* or *LIN28* were replaced with a BamHI site and then were also cloned into pCR2.1. The cDNAs without a translation termination codon were thereafter ligated with *2A* self-cleavage sequences in pBS-2A[19] with appropriate restriction enzymes to generate pBS–cDNA–2A. *c-MYC–2A* was digested with NotI and BspHI and was ligated into the NotI and NcoI sites of pBS-LIN28-2A in the same reading frame to generate the *c-MYC–LIN28–NANOG* cassette. These *cDNA–2A* or *c-MYC–2A–LIN28–2A* constructs were then ligated to another cDNA or *NANOG* in pCR2.1 with the translation termination codon in the same reading frame using appropriate restriction enzymes. These cDNA-*2A*-cDNA-stop or *c-MYC–2A–LIN28–2A–NANOG*–stop constructs were then inserted into the EcoRI site of pCXLE-EGFP. pCXLE-hOCT3/4-shp53 was constructed by inserting an shRNA expression cassette for *p53*, driven by the mouse *U6* promoter, into the BamHI site of pCXLE-hOCT3/4. The pCXLE-Fbx15-cont2 was generated by inserting the *FBXO15* cDNA into pCXLE-EGFP. Episomal vectors described previously[6] were obtained from Addgene (20922–20927).

Generation of iPSCs with episomal vectors. HDF and DP cells were cultured in DMEM supplemented with 10% FBS and mesenchymal stem cell growth medium (MSCGM), respectively. Three micrograms of expression plasmid mixtures were electroporated into 6×10^5 HDF or DP cells with Microporator (Invitrogen) with a 100-µl kit according to the manufacturer's instructions. The plasmid mixtures used in the experiments are shown in **Supplementary Table 2**. Conditions used were 1,650 V, 10 ms, 3 time pulses for HDF, and 1,800 V, 20 ms, 1 time pulse for DP cells. The cells were trypsinized 7 d after transduction, and 1×10^5 cells were re-plated onto 100-mm dishes covered with an SNL or MEF feeder layer. The culture medium was replaced the next day with primate ESC medium containing bFGF. The colonies were counted 26–32 d after plating, and those colonies similar to human ESCs were selected for further cultivation and evaluation. The pla-iPSC clones used in this study are summarized in **Supplementary Table 9**.

Characterization of pla-iPSC clones. Isolation of total RNA, RT-PCR of marker gene expression, DNA microarray, bisulfite genomic sequencing and teratoma formation were performed as previously described[17]. The primer sequences used in this study are shown in **Supplementary Table 10**. The chromosomal G-band analyses were performed at the Nihon Gene Research Laboratories. Short tandem repeat analyses were performed at Bex Co.; briefly, genomic DNAs were amplified by the PowerPlex 16 system (Promega) and were then analyzed with an ABI PRISM 3100 genetic analyzer and the GeneMapper v3.5 software program (Applied Biosystems). Differentiation of pla-iPSC clones into dopaminergic neurons was performed using the serum-free culture of embryoid body–like aggregates (SFEB) method combined with double SMAD inhibition by a BMP antagonist and an Activin/Nodal inhibitor as described elsewhere[20]. *In vitro* directed differentiation into retinal pigment epithelial cells was performed with the modified stromal cell–derived inducing activity method[21,22]. Briefly, pla-iPSCs were collected with trypsin and collagenase IV, and were treated with inhibitors for WNT and Nodal signaling under serum-free conditions. The cells were then maintained in PA6-conditioning medium for maturation.

Episomal copy-number detection. Cells cultured in 60-mm dishes were collected with a cell scraper after removing feeder cells by treatment with dissociation solution consisting of 0.25% trypsin, 1 mg ml^{-1} collagenase, 1 mM $CaCl_2$ and 20% KSR in PBS. The cells were then placed into tubes and centrifuged, and the cell pellets were lysed with 200 µl of lysis solution, containing 1× Ex Taq buffer (Takara) and 167 µg ml^{-1} proteinase K. The lysates were incubated at 55 °C for 3 h, and proteinase K was inactivated at 95 °C. The lysates were used for quantitative PCR analysis. The pCXLE-hFbx15-cont2 plasmid was used to generate a standard curve to determine the correlation between copy number and threshold cycle (Ct) values for *FBXO15* or *EBNA-1*. Then the copy number of *FBXO15* and *EBNA-1* in each iPSC sample was estimated from the observed Ct values. The cell number in each reaction was estimated by dividing the estimated copy number of *FBXO15* by two since each cell had two *FBXO15* alleles. One reaction included up to 1.2×10^4 cells. The total copy number of *EBNA-1* was measured in $\sim 5 \times 10^4$ cells by repeating six or seven reactions.

HLA typing and estimation of coverage. HLA typing of 107 DP cell lines was performed with the PCR-reverse sequence specific oligonucleotide probe (rSSOP) method using LABType SSO

(One lambda) at Repro Cell[23]. Additional HLA typing was performed with PCR-rSSOP using WAKFlow (Wakunaga Pharmaceutical) at HLA Laboratory. We performed pedigree study of 4,743 Japanese families (17,325 members) and identified 2,117 haplotypes, including interlocus recombinant haplotypes, which were detected in family studies. The haplotype frequency was calculated by direct counting on the parents in the families. Sequence-based typing was performed with AlleleSEQR (Atria Genetics) at Mitsubishi Chemical Medience Corporation.

To estimate coverage of Japanese population by HLA homozygous donors, we first calculated the frequencies of all possible combinations of the 2,117 HLA haplotypes shown in **Supplementary Table 8**. Haplotype combinations that can be covered by a given homozygous donor were then identified and their frequencies were added to estimate coverage by the homozygous donor. When one *HLA-A, HLA-B, HLA-DRB1* heterozygous individual was covered by multiple homozygous donors, we counted only once to avoid overestimation.

The expected number (EN) of each homozygous haplotype at a given population size (PS) was first calculated as; EN = (haplotype frequency)^2 × PS. EN (if EN < 1) or 1 was then summed for each homozygous haplotype to estimate the expected numbers of unique HLA haplotype donors at the given PS.

Statistical analyses. Data are shown as the mean ± s.d. Statistical significance among multiple groups was evaluated with the Steel-Dwass test.

16. McMahon, A.P. & Bradley, A. *Cell* **62**, 1073–1085 (1990).
17. Takahashi, K. *et al. Cell* **131**, 861–872 (2007).
18. Niwa, H., Yamamura, K. & Miyazaki, J. *Gene* **108**, 193–199 (1991).
19. Okita, K., Nakagawa, M., Hyenjong, H., Ichisaka, T. & Yamanaka, S. *Science* **322**, 949–953 (2008).
20. Morizane, A., Doi, D., Kikuchi, T., Nishimura, K. & Takahashi, J. *J. Neurosci. Res.* **89**, 117–126 (2010).
21. Kawasaki, H. *et al. Proc. Natl. Acad. Sci. USA* **99**, 1580–1585 (2002).
22. Osakada, F. *et al. J. Cell Sci.* **122**, 3169–3179 (2009).
23. Itoh, Y. *et al. Immunogenetics* **57**, 717–729 (2005).

doi:10.1038/nmeth.1591

Chapter 11

Tumorigenesis of Glioma-Initiating Cells: Role of Sox11

Toru Kondo

Abstract Recent studies have demonstrated that malignant tumors contain cancer-initiating cells (CICs, also known as cancer stem cells), which self-renew and are tumorigenic. Moreover, CICs are resistant to both irradiation and chemotherapy. These findings suggest that CICs are critical targets for successful cancer therapy. However, CICs have not been well characterized, due to a lack of specific markers for them. We recently established mouse glioma-initiating cell (GIC) lines, by overexpressing oncogenic $HRas^{L61}$ in p53-deficient neural cells. These cells form transplantable glioblastoma multiforme (GBM) with features of human GBM when as few as 10 cells are transplanted in vivo, suggesting that these GIC-like cells are enriched in CICs. Characterization of these GICs showed that they expressed little or no Sox11. The overexpression of exogenous Sox11 in GICs blocked their tumorigenesis by inducing their neuronal differentiation, which was accompanied by decreased levels of a novel oncogene, *plagl1*. These findings suggest that Sox11 and Plagl1 work as a tumor suppressor and oncogene, respectively, in GBM and are potential therapeutic targets.

Keywords Tumorigenesis · Glioma · Sox11 · Oncogene · Gliomagenesis · CIC

T. Kondo (✉)
Laboratory for Cell Lineage Modulation, RIKEN Center for Developmental Biology, Kobe, Japan
e-mail: tkondo@cdb.riken.jp

Introduction

During the last decade, tissue-specific stem cells were identified in almost all tissues. These cells self-renew and continuously generate the residential differentiated cells that are responsible for tissue functions and homeostasis (Weissman et al., 2001). Neural stem cells (NSCs) in the central nervous system (CNS), for example, self-renew and give rise to neurons, astrocytes, and oligodendrocytes throughout life (Gage, 2000).

The discovery of tissue-specific stem cells represented a big turning point in cancer research. The use of stem cell markers, for instance, revealed that malignant gliomas contain malignant cells that maintain the characteristics of tissue-specific stem cells (Kondo, 2006; Singh et al., 2004; Vescovi et al., 2006). Malignant gliomas also contain both proliferating cells that express NSC markers and cells that express either neuronal or glial markers, raising the possibility that these tumors contain NSC-like cancer cells. This idea is supported by the finding that malignant gliomas can arise from either NSCs or glial lineage cells (Bachoo et al., 2002; Dai et al., 2001; Uhrbom et al., 2002), such as oligodendrocyte precursor cells (OPCs) or astrocytes, which can behave like NSCs under certain conditions (Belachew et al., 2003; Doetsch et al., 1999; Kondo and Raff, 2000; Laywell et al., 2000; Nunes et al., 2003).

Additional evidence suggests that malignant tumors contain stem cell-like cancer-initiating cells (CICs, also known as cancer stem cells) (Globus and Kuhlenbeck, 1944; Hopewell and Wright, 1969; Copeland et al., 1975). Although many anti-cancer drugs are used to try to eliminate cancers, some cancer cells usually survive, and the cancer recurs, showing

M.A. Hayat (ed.), *Stem Cells and Cancer Stem Cells, Volume 1*,
DOI 10.1007/978-94-007-1709-1_11,

that the surviving cells are not only resistant to the anti-cancer drugs but also malignant. Various ATP binding cassette (ABC) transporters, such as the protein encoded by the multi-drug resistance gene (MDR), the multi-drug resistance protein (MRP), and the breast cancer resistance protein (BCRP1), contribute to the drug resistance in cancers (Gottesman et al., 2002; Wulf et al., 2001). Interestingly, some of these transporters are also expressed in many kinds of normal stem cells. BCRP1, for example, excludes the fluorescent dye Hoechst 33342, thereby identifying a side population (SP) that is enriched in stem cells (Goodell et al., 1996; Zhou et al., 2001). Together, these findings suggest that cancers might contain an SP rich in cells with the characteristics of CICs.

CIC-enriched populations can be obtained from cancers and cancer cell lines, by exploiting features common to tissue-specific stem cells, including cell-surface antigens such as CD133, their identification as side population (SP) cells, floating sphere formation assays, or a combination of these features (Kondo, 2006; Singh et al., 2004; Vescovi et al., 2006). However, CD133-negative cells and non-SP cells from tumors and cancer cell lines can also form tumors when transplanted in vivo (Mitsutake et al., 2007; Shmelkov et al., 2008). Therefore, it remains uncertain whether the existing isolation methods can identify bona fide CICs.

The overexpression of oncogenes can induce hematopoietic stem/precursor cells to transform into leukemic stem cell-like cells in culture, and the transplantation of small numbers of these cells can cause leukemias in vivo (Krivtsov and Armstrong, 2007). This observation suggests the existence of CIC-like cells in induced cancer models. Using a similar approach, we recently established an induced mouse glioma cell line, NSCL61 s. To do this, we transformed *p53*-deficient neural stem cells (NSCs) with oncogenic $HRas^{L61}$, because p53 is the most frequently mutated tumor-suppressor gene in human Glioblastoma multiforme (GBM), one of the most malignant brain tumors, and increased activation of the Ras signaling pathway is found in approximately 90% of GBM cases (Cancer Genome Atlas Research Network, 2008; Parsons et al., 2008). We analyzed NSCL61 s, human primary glioma sphere lines, and human glioma tissue samples using multiple approaches, and found that glioma-initiating cells (GICs) largely lost their *sox11* expression, but expressed *plagl1*, a transcriptional regulator of imprinting genes. In this review, I will give an overview of our recent results and discuss the future of GIC research.

Origin of Glioma Cells

The concept of CICs was first proposed several decades ago. For example, Globus and Kuhlenbeck suggested in 1944 that malignant brain tumors are generated from immature cells (NSCs or neural precursor cells) in the ventricular zone (VZ) (Globus and Kuhlenbeck, 1944); this hypothesis was subsequently proven through a number of experiments. For example, Hopewell and Wright (1969) discovered that brain tumors arose frequently from the VZ when carcinogenic pellets were randomly placed in the adult brain. Copeland and colleagues also showed that brain tumors were induced in the subventricular zone (SVZ) when mouse brains were infected with avian sarcoma viruses (Copeland et al., 1975). More recently, Doetsch et al. showed that astrocytes in the SVZ can behave like multipotent NSCs in the adult brain (Doetsch et al., 1999). Together with the knowledge that NSCs in the VZ/SVZ survive in adult animals and, unlike differentiated neural cells, proliferate throughout life, these findings suggest that NSCs in the VZ/SVZ have a higher probability of accumulating oncogenic mutations and transforming into CICs that retain the characteristics of NSCs and are malignant (Fig. 11.1). Consistent with this idea, malignant brain tumors, including GBM and medulloblastoma, are immunolabeled both for NSC markers, including Nestin, CD133, Bmi1, Sox2, Musashi1/2 and Olig2, and differentiation markers, including the neuronal marker MAP2, the astrocyte marker GFAP, and for the oligodendrocyte marker GC (Katsetos et al., 2001; Ligon et al., 2007; Toda et al., 2001).

OPCs may be the cells of origin for some gliomas. Although OPCs are committed to differentiating into oligodendrocytes in vivo, they can also differentiate into GFAP-positive astrocytes and acquire NSC characteristics, including the expression of NSC markers and multipotentiality, when cultured under specific conditions (Belachew et al., 2003; Kondo and Raff, 2000; Laywell et al., 2000; Nunes et al., 2003) (Fig. 11.1). Moreover, OPCs transformed with oncogenic HRas and c-Myc can form malignant glioma in vivo (Barnett et al., 1998).

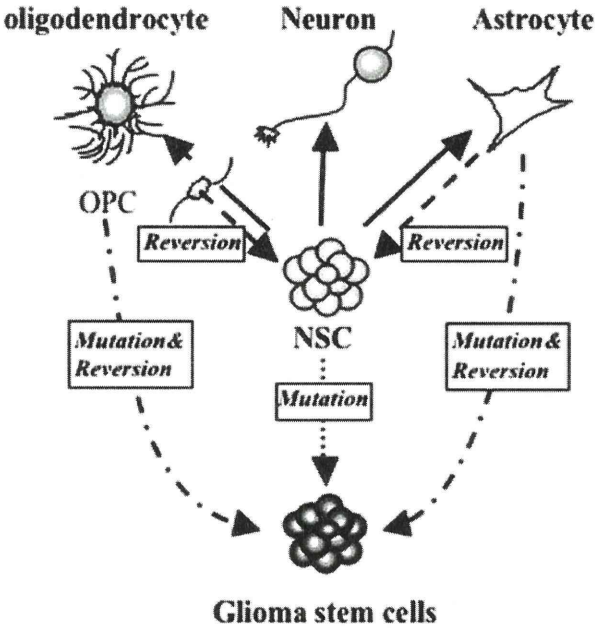

Fig. 11.1 Cell of origin for gliomagenesis. Many lines of evidence suggest that astrocytes and oligodendrocyte precursor cells, both of which can acquire multipotentiality, and NSCs are cells of origin for malignant glioma

By combining transgenic mouse technology and a retrovirus system, two groups have demonstrated that Nestin-positive NSCs and GFAP-positive astrocytes form malignant gliomas in vivo: Holland and his colleagues infected transgenic mice that expressed the avian leukosis virus (ALV) receptor under the regulation of either a *nestin* enhancer or a *gfap* promoter, with recombinant ALVs encoding oncogenic genes, such as platelet derived growth factor (PDGF) receptor beta, activated Akt, or activated Ras, and found that GBM developed in the brain (Dai et al., 2001; Uhrbom et al., 2002). De Pinho and colleagues overexpressed a constitutively active epidermal growth factor (EGF) receptor in NSCs or astrocytes with the loss of both p16/Ink4a and p19/ARF, transplanted them into the brain, and found that the cells formed high-grade gliomas (Bachoo et al., 2002). These findings suggested that NSCs and astrocytes are cells of origin for brain tumors.

GICs Induced in Mouse

It remains controversial whether GICs arise from NSCs, committed precursor cells, or differentiated neural cells. In addition, the relationship between the cell of origin for brain CICs and genetic alterations within these cells has not been elucidated, although a number of oncogenes and tumor suppressor genes are clearly associated with gliomagenesis. Now, however, it is possible to use neural lineage markers and flow cytometry to isolate neural lineage cells and examine which ones transform into CICs when overexpressing oncogenes and/or when tumor suppressor gene expression is reduced or absent. By using this strategy, we successfully generated two GIC lines, NSCL61 and OPCL61, from p53-deficient NSCs and OPCs respectively, but not from astrocytes, by overexpressing oncogenic $HRas^{L61}$ (Fig. 11.2). Both GIC lines self-renew, express NSC markers including Nestin and Sox2, and form transplantable GBM that shows hypercellularity, pleomorphism, multinuclear giant cells, mitosis, and necrosis within 2 months, even when as few as ten cells are transplanted in vivo (Hide et al., unpublished data).

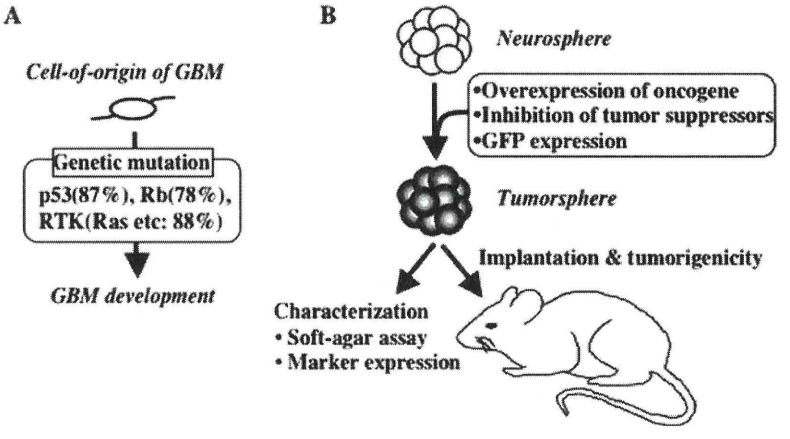

Fig. 11.2 Induced GIC model in mouse. (**a**) Glioma cells-of-origin transform into GICs by undergoing mutations for key factors involved in the p53, Rb, and/or receptor tyrosine kinase (RTK) pathways. (**b**) Induced GICs can be characterized in culture and in vivo

Sox11: A Novel Tumor Suppressor for Gliomagenesis

Given that our induced GIC lines contain both tumorigenic (GIC-like) and non-tumorigenic (non-GIC) cells, it should be possible to isolate the GIC-like cells, characterize them, and use them to identify novel therapeutic targets for GBM, by comparing their gene expression profiles with those of non-GICs. We were able to isolate both GIC and non-GIC clones from NSCL61 s by limiting dilution assays (Hide et al., 2009). We found that GIC clones proliferate much more slowly than non-GIC clones, although the mechanism is unknown. We also found that the GIC clones could be immunolabeled for NSC and glial cell markers but not for neuronal markers, whereas the non-GIC clones were largely positive for neuronal markers and lost the expression of NSC and glial markers. Moreover, a DNA microarray analysis revealed that the expression of a number of genes increased or decreased in the GIC clones compared with the non-GIC clones.

From among these genes, we chose to focus on the Sox11 transcription factor for the following reasons. First, Sox11 is not expressed in primary human glioma spheres, which are rich in GICs. Second, Sox11 induces the expression of the neuronal markers MAP2 and βIII tubulin in proliferating neural precursors cells (Bergsland et al., 2006). Third, the overexpression of a dominant-negative form of Sox11 blocks neuronal differentiation (Bergsland et al., 2006). Fourth, the National Cancer Institute's Repository for Molecular Brain Neoplasia Data (REMBRANDT) database (Madhavan et al., 2009) revealed that a downregulation of *sox11* mRNA is correlated with a significant decrease in the survival of glioma patients. Fifth, we found that human primary GBMs express *sox11* mRNA and Sox11 protein, whereas the recurrent GBMs lose Sox11. Together, these findings suggest that Sox11 may inhibit malignancy in GICs by inducing their neuronal differentiation (Fig. 11.3). In support of this idea, we found that the overexpression of Sox11 inhibits the tumorigenesis of GICs by inducing their neuronal differentiation and increases the susceptibility of GICs to chemotherapy. In contrast, the knockdown of *sox11* induces non-GIC clones to become tumorigenic (Hide et al., 2009).

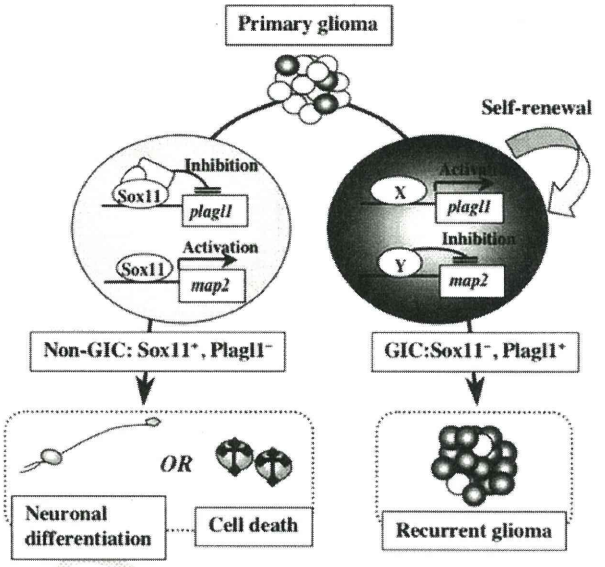

Fig. 11.3 Model of tumorigenesis by $Sox11^{-}/Plagl1^{+}$ GICs. Primary GBM contains both GICs, which are $Sox11^{+}$ and $Plagl1^{-}$, and non-GICs, which are $Sox11^{-}$ and $Plagl1^{+}$. Non-GICs probably differentiate into neurons and are sensitive to chemotherapy. Recurrent GBMs largely consist of GICs that are resistant to differentiation inducers and chemotherapy

Plagl1: A Novel Oncogene for Gliomagenesis

How does Sox11 inhibit the tumorigenesis of GICs? To identify targets of Sox11 in GICs, we analyzed the gene expression differences between non-Sox11-expressing and exogenous Sox11-expressing GICs using DNA microarray analysis and selected several genes whose expression was significantly affected by *sox11* overexpression. We focused on Pleiomorphic adenoma gene-like 1 (Plagl1) for the following reasons. First, *plagl1* is expressed in the neural stem/progenitor cells of developing neuroepithelial cells and decreases upon differentiation (Valente et al., 2005). Second, we found that *plagl1* is expressed in malignant human gliomas as well as in human GICs, although it was thought to be a tumor suppressor candidate (Van Dyck et al., 2007). Third, Plagl1 regulates several imprinted genes, including Insulin-like growth factor 2 (Igf2), H19, and Delta-like 1 (Dlk1), all of which are involved in tumorigenesis as well as early development (Varrault et al., 2006). Fourth, the REMBRANDT database revealed that glioma patients with downregulated *plagl1* mRNA show increased

survival rates compared to patients with intermediate levels of *plagl1* expression. Together, these data suggest that Plagl1 plays an important role in GICs.

We found that Sox11 can block the *plagl1* expression in GICs by binding to the 5' promoter region of the gene. Moreover, the overexpression of Plagl1 induces non-GICs to become tumorigenic, while its knockdown blocks the tumorigenicity of GICs. Collectively, these results suggest that Plagl1 plays an important role in the tumorigenicity of GICs (Fig. 11.3).

Discussion

Although tumors are the primary sources of CICs, induced CICs are a useful alternative source for their characterization, because CICs cannot presently be purified from tumors. In addition, induced CIC models can be used to identify experimentally the cell-of-origin of the cancer, the responsible oncogenic mutation, and the relationship between them. Indeed, we demonstrated that the overexpression of $HRas^{L61}$ induced p53-deficient NSCs to transform into GICs (Hide et al., 2009), consistent with recent findings that mutations in the p53 and RTK pathways as well as the retinoblastoma (Rb) pathway are critical for human GBM development (Cancer Genome Atlas Research Network, 2008; Parsons et al., 2008). Moreover, we successfully separated both tumorigenic and non-tumorigenic clones from induced GIC lines using limiting dilution methods and identified many genes, including Sox11 and Plagl1, that are up- or down-regulated in tumorigenic clones (Hide et al., 2009).

Sox11 was originally thought to be involved in tumor induction, because it is expressed in many malignant human gliomas. However, we showed that human primary glioma sphere cells and recurrent glioma as well as mouse tumorigenic clones are largely negative for Sox11, whereas primary gliomas express Sox11. On the other hand, Plagl1 was thought to be a tumor suppressor regulating both cell-cycle arrest and apoptosis. We found, however, that plagl1 is predominantly expressed in tumorigenic clones and human glioma sphere cells, that the overexpression of *plagl1* transforms non-GIC-like cells into GICs, and that its knock-down inhibits the tumorigenicity of NSCL61 s. Thus, it is important to establish a number of induced GIC models and examine their characteristics to identify therapeutic targets and develop related treatment methods.

References

Bachoo RM, Maher EA, Ligon KL, Sharpless NE, Chan SS, You MJ, Tang Y, DeFrances J, Stover E, Weissleder R, Rowitch DH, Louis DN, DePinho RA (2002) Epidermal growth factor receptor and Ink4a/Arf: convergent mechanisms governing terminal differentiation and transformation along the neural stem cell to astrocyte axis. Cancer Cell 1:267–277

Barnett SC, Robertson L, Graham D, Allan D, Rampling R (1998) Oligodendrocyte-type-2 astrocyte (O-2A) progenitor cells transformed with c-myc and H-ras form high-grade glioma after stereotactic injection into the rat brain. Carcinogenesis 19:1529–1537

Belachew S, Chittajallu R, Aguirre AA, Yuan X, Kirby M, Anderson S, Gallo V (2003) Postnatal NG2 proteoglycan–expressing progenitor cells are intrinsically multipotent and generate functional neurons. J Cell Biol 161:169–186

Bergsland M, Werme M, Malewicz M, Perlmann T, Muhr J (2006) The establishment of neuronal properties is controlled by Sox4 and Sox11. Genes Dev 20:3475–3486

Cancer Genome Atlas Research Network (2008) Comprehensive genomic characterization defines human glioblastoma genes and core pathways. Nature 455:1061–1068

Copeland DD, Vogel FS, Bigner DD (1975) The induction of intracranial neoplasms by the inoculation of avian sarcoma virus in perinatal and adult rats. J Neuropathol Exp Neurol 34:340–358

Dai C, Celestino JC, Okada Y, Louis DN, Fuller GN, Holland EC (2001) PDGF autocrine stimulation dedifferentiates cultured astrocytes and induces oligodendrogliomas and oligoastrocytomas from neural progenitors and astrocytes in vivo. Genes Dev 15:1913–1925

Doetsch F, Caille I, Lim DA, Garcia-Verdugo JM, Alvarez-Buylla A (1999) Subventricular zone astrocytes are neural stem cells in the adult mammalian brain. Cell 97: 703–716

Gage F (2000) Mammalian neural stem cells. Science 287: 1433–1438

Globus JH, Kuhlenbeck H (1944) The subependymal cell plate (matrix) and its relationship to brain tumors of the ependymal type. J Neuropathol Exp Neurol 3:1–35

Goodell MA, Brose K, Paradis G, Conner AS, Mulligan RC (1996) Isolation and functional properties of murine hematopoietic stem cells that are replicating in vivo. J Exp Med 183:1797–1806

Gottesman MM, Fojo T, Bates SE (2002) Multidrug resistance in cancer: role of ATP-dependent transporters. Nat Rev Cancer 2:48–58

Hide T, Takezaki T, Nakatani Y, Nakamura H, Kuratsu J, Kondo T (2009) Sox11 prevents tumorigenesis of glioma-initiating cells by inducing neuronal differentiation. Cancer Res 15:7953–7959

Hopewell JW, Wright EA (1969) The importance of implantation site in cerebral carcinogenesis in rats. Cancer Res 29:1927–1932

Katsetos CD, Spandou E, Legido A, Taylor ML, Zanelli SA, de Chadarevian JP, Christakos S, Mishra OP, Delivoria-Papadopoulos M (2001) Localization of the neuronal class III beta-tubulin in oligodendrogliomas: comparison with Ki-67 proliferative index and 1p/19q status. J Neuropathol Exp Neurol 61:307–320

Kondo T (2006) Brain cancer stem-like cells. Eur J Cancer 42:1237–1242

Kondo T, Raff M (2000) Oligodendrocyte precursor cells reprogrammed to become multipotential CNS stem cells. Science 289:1754–1757

Krivtsov AV, Armstrong SA (2007) MLL translocations, histone modifications and leukaemia stem-cell development. Nat Rev Cancer 7:823–833

Laywell ED, Rakic P, Kukekov VG, Holland EC, Steindler DA (2000) Identification of a multipotent astrocytic stem cell in the immature and adult mouse brain. Proc Natl Acad Sci USA 97:13889–13894

Ligon KL, Huillard E, Mehta S, Kesari S, Liu H, Alberta JA, Bachoo RM, Kane M, Louis DN, DePinho RA, Anderson DJ, Stiles CD, Rowitch DH (2007) Olig2-regulated lineage-restricted pathway controls replication competence in neural stem cells and malignant glioma. Neuron 53:503–517

Madhavan S, Zenklusen JC, Kotliarov Y, Sahni H, Fine HA, Buetow K (2009) Rembrandt: helping personalized medicine become a reality through integrative translational research. Mol Cancer Res 7:157–167

Mitsutake N, Iwao A, Nagai K, Namba H, Ohtsuru A, Saenko V, Yamashita S (2007) Characterization of side population in thyroid cancer cell lines: cancer stem-like cells are enriched partly but not exclusively. Endocrinology 148: 1797–1803

Nunes MC, Roy NS, Keyoung HM, Goodman RR, McKhann II G, Jiang L, Kang J, Nedergaard M, Goldman SA (2003) Identification and isolation of multipotential neural progenitor cells from the subcortical white matter of the adult human brain. Nat Med 9:439–447

Parsons DW, Jones S, Zhang X, Lin JC, Leary RJ, Angenendt P, Mankoo P, Carter H, Siu IM, Gallia GL, Olivi A, McLendon R, Rasheed BA, Keir S, Nikolskaya T, Nikolsky Y, Busam DA, Tekleab H, Diaz LA Jr, Hartigan J, Smith DR, Strausberg RL, Marie SK, Shinjo SM, Yan H, Riggins GJ, Bigner DD, Karchin R, Papadopoulos N, Parmigiani G, Vogelstein B, Velculescu VE, Kinzler KW (2008) An integrated genomic analysis of human glioblastoma multiforme. Science 321:1807–1812

Shmelkov SV, Butler JM, Hooper AT, Hormigo A, Kushner J, Milde T, St Clair R, Baljevic M, White I, Jin DK, Chadburn A, Murphy AJ, Valenzuela DM, Gale NW, Thurston G, Yancopoulos GD, D'Angelica M, Kemeny N, Lyden D, Rafii S (2008) CD133 expression is not restricted to stem cells, and both CD133+ and CD133– metastatic colon cancer cells initiate tumors. J Clin Invest 118:2111–2120

Singh SK, Clarke ID, Hide T, Dirks PB (2004) Cancer stem cells in nervous system tumors. Oncogene 23:7267–7273

Toda M, Iizuka Y, Yu W, Imai T, Ikeda E, Yoshida K, Kawase T, Kawakami Y, Okano H, Uyemura K (2001) Expression of the neural RNA-binding protein Musashi1 in human gliomas. Glia 34:1–7

Uhrbom L, Dai C, Celestino JC, Rosenblum MK, Fuller GN, Holland EC (2002) Ink4a-Arf loss cooperates with KRas activation in astrocytes and neural progenitors to generate glioblastomas of various morphologies depending on activated Akt. Cancer Res 62:5551–5558

Valente T, Junyent F, Auladell C (2005) Zac1 is expressed in progenitor/stem cells of the neuroectoderm and mesoderm during embryogenesis: differential phenotype of the Zac1-expressing cells during development. Dev Dyn 233:667–679

Van Dyck F, Declercq J, Braem CV, Van de Ven WJ (2007) PLAG1, the prototype of the PLAG gene family: versatility in tumour development (review). Int J Oncol 30:765–774

Varrault A, Gueydan C, Delalbre A, Bellmann A, Houssami S, Aknin C, Severac D, Chotard L, Kahli M, Le Digarcher A, Pavlidis P, Journot L (2006) Zac1 regulates an imprinted gene network critically involved in the control of embryonic growth. Dev Cell 11:711–722

Vescovi AL, Galli R, Reynolds BA (2006) Brain tumour stem cells. Nat Rev Cancer 6:425–436

Weissman IL, Anderson DJ, Gage F (2001) Stem and progenitor cells: origins, phenotypes, lineage commitments, and transdifferentiations. Annu Rev Cell Dev Biol. 17: 387–403

Wulf GG, Wang RY, Kuehnle I, Weidner D, Marini F, Brenner MK, Andreeff M, Goodell MA (2001) A leukemic stem cell with intrinsic drug efflux capacity in acute myeloid leukemia. Blood 98:1166–1173

Zhou S, Schuetz JD, Bunting KD, Colapietro AM, Sampath J, Morris JJ, Lagutina I, Grosveld GC, Osawa M, Nakauchi H, Sorrentino BP (2001) The ABC transporter Bcrp1/ABCG2 is expressed in a wide variety of stem cells and is a molecular determinant of the side-population phenotype. Nat Med 7:1028–1034

Chapter 2
Stem Cells and Cancer Stem Cells: New Insights

Toru Kondo

Prologue to Cancer Stem Cell Research

Although the concept of the cancer stem cell (CSC) was advocated more than several decades ahead, it was not accepted widely due to the lack of a direct proof method. However, recent progresses in the stem cell biology and developmental biology revealed that cancers contain the hierarchy similar to normal tissues and that only CSCs in tumors have a strong self-renewal capability and are malignant (Fig. 2.1) (Reya et al. 2001). It is thought that the existence ratio of CSCs is several percent or less in tumors and cancer cell lines and the other cells (non-CSCs) are either cancer precursor cells, which have limited proliferation ability, or nondividing cancer cells. Together these findings suggest that characterization of CSCs is essential for the curable cancer therapy.

Definition of CSCs

CSCs were initially defined by their extensive self-renewal capacity, tumorigenicity, and multipotentiality. As a number of oncogenes, including *inhibitor of differentiation* (*Id*), *hairy and enhancer of splits* (*Hes*) and *Notch*, are expressed in CSCs as well as tissue-specific stem cells (TSCs) and block cell differentiation, it remains uncertain as to whether CSCs actually give rise to multilineage cells. Further evidence also exists suggesting that cancer cells co-express a number of lineage-specific

T. Kondo (✉)
Laboratory for Cell Lineage Modulation, RIKEN Center for Developmental Biology, 2-2-3 Minatojima-Minamimachi, Chuo-ku, Kobe, Hyogo 650-0047, Japan

Department of Stem Cell Biology, Ehime University Proteo-Medicine Research Center, Shigenobu, Toon, Ehime 791-0295, Japan
e-mail: tkondo@m.ehime-u.ac.jp

R. Scatena et al. (eds.), *Advances in Cancer Stem Cell Biology*,
DOI 10.1007/978-1-4614-0809-3_2,

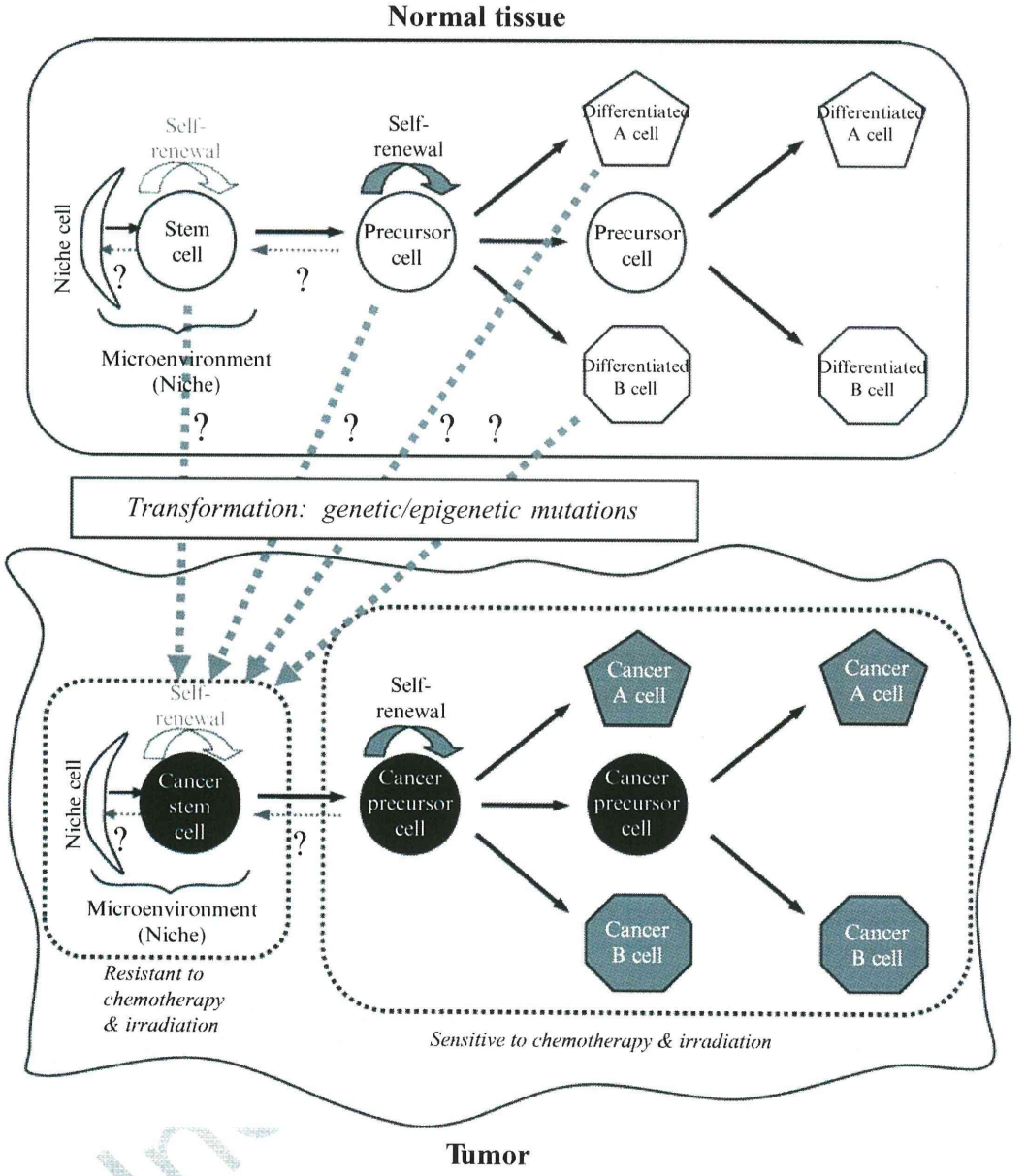

Fig. 2.1 Similarity between normal tissue and tumor. Tumors as well as normal tissues are likely to consist of small number of stem cells that have self-renewal capability and multipotentiality, precursor cells that have limited proliferative potency, and differentiated cells. CSCs are thought to be transformed from TSCs, precursor cells and/or differentiated cells by genetic/epigenetic mutations. Moreover, CSCs exist in special microenvironment "niche" and seem to keep their resistance to a variety of anti-cancer treatment methods

markers, each of which is exclusively expressed in normal differentiated cells, such as neurofilaments in neurons, glial fibrillary acidic protein in astrocytes and galactocerebrocide in oligodendrocytes, raising the question of whether such lineage-marker positive cells are in fact differentiated cells. Seen against this light then the obvious definition that can be applied to CSCs might be their unlimited self-renewal, expression of TSC markers, and tumorigenicity.

Cell-of-Origin of CSCs

Cancers have traditionally been thought to arise from either differentiated cells or their proliferating precursor cells, which have acquired oncogenic mutations. Since stem cells have been discovered in adult tissues, however, it has been suggested that TSCs might be a principal target of such mutations (Fig. 2.1). This speculation is supported by a number of different findings: First, it is likely that cancers arise from epithelia, which are in contact with the external environment and contain a wide variety of TSCs. Second, many cancers have been immunolabeled for TSC markers and for differentiation markers. Third, while TSCs survive and continue to proliferate throughout life, differentiated cells do not, suggesting that TSCs are more susceptible to accumulating oncogenic mutations. Finally, stem cells and precursor cells, which are transformed with oncogenic genes, have been shown to as developing cancer in vivo. Together, these findings suggest that either TSCs or amplifying precursor cells can be seen as the origin of malignant tumors.

[AU1]

Characteristics of CSCs

Resistance to Chemotherapy

A number of anti-cancer drugs have been successful in eliminating cancers; however, some cancer cells survive and the cancer recurs, indicating that the surviving cells are not only resistant to such anti-cancer drugs but are also malignant (Gottesman et al. 2002; Szakacs et al. 2006). It has been shown that glutathione and its related enzyme apparatus, topoisomerase II, O6-methylguanine-DNA-methyltransferase, dihydrofolate reductase, metallothioneins, and various ATP-binding cassette (ABC) transporters, such as the protein encoded by the multidrug resistant gene (MDR), the multidrug resistant protein (MRP), and the breast cancer resistant protein (BCRP1), contribute to such drug resistance in cancers. It is crucial to investigate relationship between CSCs and these factors.

Resistance to Irradiation

Irradiation is one of the most effective therapies for malignant tumors; however, a small population of cancerous cells tends to survive and cause tumor recurrence, suggesting that CSCs are radioresistant. Recently, Bao et al. (2006) have revealed that CD133-positive glioblastoma CSCs are much more resistant to irradiation than CD133-negative cells.

Invasion/Metastatic Activity

One characteristic of malignant tumor cells is their ability to invade and disseminate into normal tissue and to metastasize into other tissues. Some of the infiltrating cancer cells cannot be removed by surgical operation and causes recurrence, suggesting that CSCs retain high invasion activity. In fact, it has demonstrated that CD133-positive cancer cells highly express CD44 and chemokine receptor CXCR4, both of which mediate cell migration (Hermann et al. 2007; Liu et al. 2006).

Niche for CSCs

The number of TSCs is precisely regulated by both intrinsic mechanism and extracellular signals derived from specialized microenvironment "niche." For example, it was demonstrated that niche provides a limited number of physical anchoring sites, including beta1-integrin and N-cadherin, for TSCs and secretes both growth factors and anti-growth factors, including Wnt, FGF, hedgehog (Hh), bone morphogenic proteins, and Notch (Li and Neaves 2006; Moore and Lemischka 2006). Hypoxia is also shown to be essential for the maintenance of stemness, tumorigenesis, and resistance to anti-cancer treatments, chemotherapy and irradiation (Das et al. 2008; Matsumoto et al. 2009). Moreover, it was shown that the ablation of such niche results in loss of TSCs. It seems likely that CSCs also need niche for tumorigenesis. Kaplan and his colleagues have elegantly demonstrated that bone marrow-derived progenitors form the pre-metastatic niche in the tumor-specific pre-metastatic sites before cancer cells arrive and that the ablation of the niche prevents tumor metastasis (Kaplan et al. 2005). However, since transplanted cancer cells form tumors in any area in vivo, CSCs might be independent of the niche regulation or have a capability to make a new niche by recruiting bone marrow stem cells and other component cells.

Preparation of CSCs

The following methods are commonly used to prepare CSCs from cancers and cancer cell lines using the common characteristics of TSCs, such as cell surface markers, side population (SP), aldehyde dehydrogenase activity (ALDH), and/or a floating sphere formation.

Cell Surface Markers

Dick and colleagues have been able to show that the acute myeloid leukemia (AML)-initiating cells are found in primitive $CD34^+$ and $CD38^-$ populations, in which hematopoietic stem cells are enriched (Bonnet and Dick 1997; Lapidot et al. 1994).

Al-Hajj et al. have successfully separated tumorigenic breast CSCs from mammary tumors and breast cancer cell lines as $CD44^+$ $CD24^{-/low}$ $Lineage^-$ cells. As few as 100 $CD44^+$ $CD24^{-/low}$ $Lineage^-$ cells formed tumors in NOD/SCID mice, while tens of thousands of other cancer cell populations did not (Al-Hajj et al. 2003; Ponti et al. 2005). Another study by Singh et al. reported their success in separating brain CSCs from human medulloblastoma and glioblastoma multiforme (GBM) using an anti-CD133 antibody that recognizes a variety of different stem cells. Here, as few as 100 $CD133^+$ GBM cells, although not $CD133^-$ cells, formed tumors in NOD-SCID brain (Singh et al. 2004). It has also revealed that colon CSCs are enriched in a $CD133^+$ population (O'brien et al. 2007; Ricci-Vitiani et al. 2007). This is in addition to prostate CSCs being found to be enriched in $CD44^+alpha2beta1^{hi}CD133^+$ (Collins et al. 2005). Very recent studies have shown that CD15, also known as stage-specific embryonic antigen 1 (SSEA1) or Lewis X (LeX), is a general CSC marker on glioblastoma multiforme (GBM) and medulloblastoma (Reed et al. 2009; Son et al. 2009; Ward et al. 2009). It therefore seems likely that cell surface markers, such as CD133, are useful in separating CSCs from many types of tumors.

[AU2]

Side Population

It was revealed that cancer cells, as well as many kinds of normal stem cells, express a number of ABC transporters. BCRP1, for example, excludes the fluorescent dye Hoechst 33342, identifying a side population (SP) (Goodell et al. 1996), which is enriched for the various types of TSCs, although some research has shown that TSCs exist in both SP and non-SP and that SP cells do not express stem cell markers (Mitsutake et al. 2007; Morita et al. 2006). A number of research groups have found that some established cancer cell lines, which have been maintained in culture for decades, and tumors, such as AML, neuroblastoma, nasopharyngeal carcinoma, and ovarian cancer, contain a small SP. These studies have demonstrated that SP cells – but not non-SP cells – self-renew in culture, are resistant to anti-cancer drugs including Mitoxantrone, and form tumors when transplanted in vivo (Haraguchi et al. 2006; Hirschmann-Jax et al. 2004; Kondo et al. 2004; Patrawala et al. 2005; Ponti et al. 2005; Szotek et al. 2006). However, since many cancer cell lines do not contain any SP fraction and non-SP cells in some cancer cell lines likely generate SP fraction during culture, it is needed to evaluate whether SP is a general method to prepare CSCs.

Aldehyde Dehydrogenase Activity

ALDH is another detoxifying enzyme oxidizing intracellular aldehydes to carboxylic acids and blocking alkylating agents. Since it has been shown that ALDH increases in TSCs (Jones et al. 1995; Cai et al. 2004), it is now possible to identify and purify

many types of TSCs, including hematopoietic stem cells and neural stem cells (NSCs), using fluorescent substrates of this enzyme and flow cytometry. There is increasing evidence that many types of CSCs strongly express ALDH and can be purified from tumors and cancer cell lines (Ginestier et al. 2007; Korkaya et al. 2008; Pearce et al. 2005).

Sphere Formation Assay

An increasing evidence points to the fact that CSCs as well as TSCs, such as NSCs and mammary gland stem cells, can form floating aggregates (tumor spheres) and be enriched in the spheres when cultured in serum-free medium with proper mitogens, such as bFGF and EGF (Fig. 2.3c) (Haraguchi et al. 2006; Hirschmann-Jax et al. 2004; Kondo et al. 2004; Ponti et al. 2005). Although many CSC researchers use sphere formation methods to concentrate their CSCs in culture, monolayer culture method might be better used to characterize CSCs as monolayer-cultured CSCs can be expanded as a homogenous population (Pollard et al. 2009). [AU3]

Signaling Pathways Involved in CSC Maintenance

Since genetic alterations cause TSCs, amplifying precursors, or differentiated cells to transform to CSCs, it is important to classify the relationship between genetic alterations and tumor phenotype and malignancy.

p53 Pathway

It is well known that the loss of p53 function promotes the accelerated cell proliferation and malignant transformation (Toledo and Wahl 2006). Indeed, it was shown that over 65% of human glioma contains TP53 gene deletion and mutation (Kleihues and Ohgaki 1999). Moreover, additional evidences also indicated that other p53 signaling factors, including Murin-double-minute 2 (MDM2), which binds to, destabilizes, and inactivates p53, and chromodomain helicase DNA-binding domain 5 (Chd5), which regulates cell proliferation, cellular senescence, apoptosis, and tumorigenesis, are mutated in malignant glioma (Bagchi et al. 2007; Kleihues and Ohgaki 1999; Reifenberger et al. 1993; Toledo and Wahl 2006) In total, it was revealed that about 90% of human glioma have mutations in p53 signaling pathway (Cancer Genome Atlas Research Network 2008; Parsons et al. 2008). Although the effector molecule of p53 pathway is the p21 cyclin-dependent kinase (cdk) inhibitor that regulates progression of cells through the G1 cell-cycle phase, it has not been demonstrated that p21 gene itself is an oncogenic target in human cancers.